Fronto-striatal connections in the human brain: A probabilistic diffusion tractography study

Sandra E. Leh [a,*], Alain Ptito [a], M. Mallar Chakravarty [a], Antonio P. Strafella [a,b]

[a] Montreal Neurological Institute and Hospital, McGill University, Canada
[b] Toronto Western Hospital-Research Institute, CAMH-PET centre, University of Toronto, Canada

Abstract

Anatomical studies in animals have described multiple striatal circuits and suggested that sub-components of the striatum, although functionally related, project to distinct cortical areas. To date, anatomical investigations in humans have been limited by methodological constraints such that most of our knowledge of fronto-striatal networks relies on nonhuman primate studies. To better identify the fronto-striatal pathways in the human brain, we used Diffusion Tensor Imaging (DTI) tractography to reconstruct neural connections between the frontal cortex and the caudate nucleus and putamen in vivo. We demonstrate that the human caudate nucleus is interconnected with the prefrontal cortex, inferior and middle temporal gyrus, frontal eye fields, cerebellum and thalamus; the putamen is interconnected with the prefrontal cortex, primary motor area, primary somatosensory cortex, supplementary motor area, premotor area, cerebellum and thalamus. A connectivity-based seed classification analysis identified connections between the dorsolateral prefrontal areas (DLPFC) and the dorsal-posterior caudate nucleus and between the ventrolateral prefrontal areas (VLPFC) and the ventral-anterior caudate nucleus. For the putamen, connections exist between the supplementary motor area (SMA) and dorsal-posterior putamen while the premotor area projects to medial putamen, and the primary motor area to the lateral putamen. Identifying the anatomical organization of the fronto-striatal network has important implications for understanding basal ganglia function and associated disease processes.
© 2007 Elsevier Ireland Ltd. All rights reserved.

Keywords: Caudate; Putamen; Frontal connectivity; Motor connectivity; Diffusion tensor imaging (DTI) tractography; Humans

The striatum is the main entry point of cortical information to the basal ganglia and it receives afferents from anatomically and functionally different areas of the cerebral cortex.

According to the current model of basal ganglia function, cortical information is processed in the basal ganglia nuclei, which in turn send projections back via the thalamus to the cortex ('cortico-basal ganglia loop') [2,1]. To date, there are two opposing views regarding the organization of this loop. The "information-funneling" hypothesis emphasizes the convergent nature of cortico-striatal projections and subsequent striato-pallidal and striato-nigral projections [28]. In contrast, the "parallel-processing" hypothesis proposes that signals originating from functionally distinct cortical areas are processed in separate striatal territories and remain segregated in the striato-pallidal/nigral projection [2,1,45]. At present, our knowledge of the functional organization of cortico-striatal networks originates largely from animal experiments [20,21,40,46]. Possibly because of evolutionary anatomical differences, these animal models do not fully describe the human fronto-striatal networks; yet, these differences may have important functional and clinical implications [20,21,37,40,46].

In the present study, we used Diffusion Tensor Imaging (DTI) tractography and a connectivity-based seed classification analysis to investigate the anatomical distribution of cortico-striatal pathways. This robust technique has been successful in the investigation of subcortical [13] and cortical connections [14,38] in humans.

We acquired DTI data from six healthy subjects in whom the putamen and caudate were defined three-dimensionally on each subject's T1-weighted image using atlas warping techniques. In the first part of this study, carried out to investigate the segregation of different striatal circuits, probabilistic fiber tracking was initiated from both structures and displayed in a population map, in MNI standard stereotaxic space. This analysis permitted

* Corresponding author at: Neuropsychology/Cognitive Neuroscience Unit, Montreal Neurological Institute, 3801 University Street, Montreal, Qc., Canada, H3A, 2B4. Tel.: +1 514 398 2993; fax: +1 514 398 1338.
E-mail address: sandra@bic.mni.mcgill.ca (S.E. Leh).

reconstruction of the connectivity of the caudate and putamen and allowed tracking of all subcortical and cortical fiber connections from every voxel predefined in a seed mask prior to analysis. In the second part of the study, a connectivity-based seed classification analysis on the putamen and caudate was carried out to examine the cortical segregation of striatal pathways, in particular putamen pathways linked to motor areas, and caudate pathways linked to prefrontal areas. With this analysis, functionally distinct subunits of the caudate and putamen were identified. By generating connectivity distributions from every voxel within the caudate and putamen, the probability of connection from every voxel within these structures to each of the predefined cortical areas was computed.

Six healthy control subjects (age range: 24–36 years) who had no history of neurological or psychiatric disorders were recruited. All gave informed written consent in accordance with ethical approval from the Montreal Neurological Hospital and Institute Research Ethics Board.

A 1.5 T Siemens Sonata scanner at the Brain Imaging Centre of the Montreal Neurological Institute (MNI) was used to obtain T_1–weighted anatomical MRI images and diffusion-weighted images. Diffusion-weighted images were acquired by using echo-planar imaging (EPI) with a standard head coil (repetition time 9300 ms, echo time 94 ms, flip angle $90°$, slice thickness = 2.2 mm, number of slices 60, in-plane resolution 2.1875 mm × 2.1875 mm, acquisition time approximately 9:30 min). Diffusion weighting was performed along 60 independent directions, with a b-value of 1000 s/mm^2 and a reference image with no diffusion weighting was also obtained.

Diffusion-weighted raw data were first corrected for eddy current distortions and motion artefacts. We then skull-stripped the T_1–images and fit diffusion tensors at each voxel independently of the data and co-registered diffusion-weighted images to the anatomical image using a six-parameter transform. Diffusion modelling, probabilistic tractography and a connectivity-based seed classification analysis were carried out using the FMRIB Diffusion Toolbox (FDT, version 1.0), which allows for an estimation of the most probable location of a pathway from a seed point using Bayesian techniques (FMRIB Software Library (FSL); www.fmrib.ox.ac.uk/fsl).

A digital atlas of the basal ganglia and thalamus was used [4] to create a seed mask of the caudate and putamen on each subject's left and right hemisphere T1-weighted image (Fig. 1II). This atlas was developed from a set of high-resolution histology sliced coronally. The reconstructed data set has an in plane voxel-to-voxel spacing of 0.034 mm while the original slice-to-slice thickness is 0.7 mm. It comes in multiple representations and was reconstructed using optimized nonlinear slice-by-slice morphological and intensity correction techniques.

The final atlas exists in multiple representations: The original reconstructed histological volume, a voxel-label-atlas where each structure is assigned a unique label to properly identify it, and a 3D geometric atlas. The atlas was warped onto a high-resolution, high signal-to-noise ratio template known as the Colin27-MRI-average using a pseudo-MRI derived from the voxel-label-atlas. The atlas-to-template nonlinear transfor-

mation was estimated using the ANIMAL algorithm [6]. The ANIMAL algorithm matches a source volume to a target volume by estimating a deformation field of local translations defined on a set of equally spaced nodes which maximizes the similarity between the source and target volumes. The accuracy of this warp and the anatomical definitions on the Colin27 template was compared against manual segmentations [5].

The right and left caudate and putamen of each subject (target volume) were defined as a volume of interest on the atlas (source volume). A high-resolution nonlinear transformation was estimated from the atlas to fit each subject using the parameters identified in Fig. 1I. The transformation is estimated in a hierarchical fashion where large deformations are estimated first and used as the input for the estimation of smaller, more refined transformations. All transformations are estimated on unblurred data (as an effective blurring is done in the subsampling methods used within ANIMAL). The stiffness, weight, and similarity parameters used were those identified in an optimization by Robbins et al. [35]. The final transformation, defined on a grid where local translations have a 1 mm isotropic spacing, was then applied to the mask of the caudate and putamen for the DTI tractography of each subject.

Fibre tracking was initiated from all voxels within the seed masks to generate 5000 streamline samples, with a steplength of 0.5 mm and a curvature threshold of 0.2. Anatomical images were transformed to standard space using the MNI coordinates with a 12-point transformation (MNI 152 brain). Out of the 5000 samples generated from each seed voxel, raw tracts were thresholded at least at 20 samples in order to remove voxels with very low connectivity probability [13]. The results were then binarised and summed across subject. The results are displayed as a population map, showing only reconstructed tracts that were present in at least 50% of the subjects (Fig. 2).

Two separate analyses were performed: (1) a connectivity-based seed qualification analysis of the caudate with the dorsolateral prefrontal cortex (DLPFC) and ventrolateral prefrontal cortex (VLPFC); and, (2) a connectivity-based seed qualification analysis of the putamen with supplementary motor area (SMA), premotor area and primary motor area. The regions of interest (seed masks) were identical in size across subjects (150 voxels). A connectivity-based seed qualification analysis and a hard segmentation on the outputs of the seed to targets were performed to generate segmentation.

The VLPFC, DLPFC, SMA, premotor area and the hand-knob area of the primary motor area were defined on each of the subject's T1-weighted image of the left and right hemisphere by using previously described landmark localizations (VLPFC: [31]; DLPFC: [30]; SMA: [27,47,48]; premotor: [3]; primary motor area: [53]. Within these areas, 150 voxels were hand-painted and included to create the seed mask.

Seed masks for the putamen and caudate were defined on each of the subject's T1-weighted image using the atlas warping techniques described above. Fibre tracking was initiated from all voxels within the seed masks. Reconstructed caudate (Fig. 2A–F) and putamen tracts (Fig. 2G–N) are displayed as a population map. Only tracts that were present in at least 50% of the subjects are shown in order to permit visualization of

I Step	Step Size (mm)	Sub-Lattice Diameter (mm)	Sub-Lattice	Iterations
1	4	8	8	15
2	2	6	8	15
3	1	6	6	15
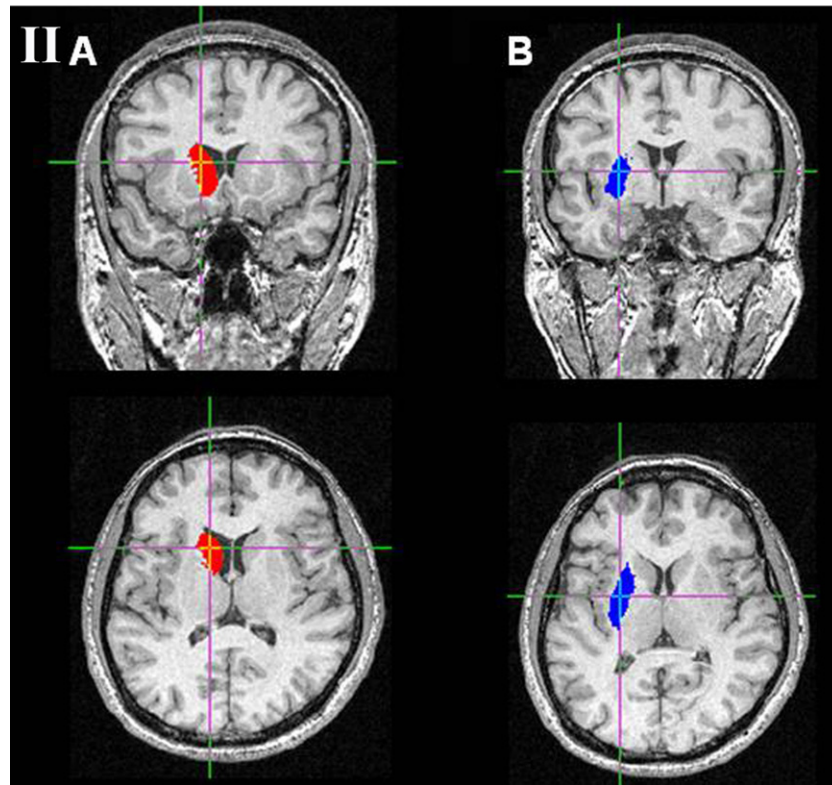
Fig. 1. (I) Atlas-to-subject warping parameters. (II) Caudate and putamen seed mask. Atlas was warped to a high resolution, high signal-to-noise ratio template. The caudate and putamen were extracted from the atlas and the atlas-to-subject transformation estimated (ANIMAL) for each subject was applied to the mask of the caudate and putamen to fit it properly to each subject (caudate, (A) red; putamen, (B) blue).

inter-subject variability. The reconstructed tracts of Fig. 2 show very low across-subject variability and were present in all of the subjects as indicated by the color yellow. Tractography of the right and left caudate showed nearly identical ipsilateral connections (e.g. Fig. 2F). Similarly, all of the reconstructed right and left putamen tracts projected to identical ipsilateral areas (e.g. Fig. 2N). For simplicity we decided to present only left putamen and caudate tracts, although the coordinates of the right and left putamen/caudate tracts are given below.

Reconstructed tracts of the left and right caudate projected ipsilaterally to the prefrontal cortex (A; $x = \pm 20$, $y = 54$, $z = 6$, area 10; $x = \pm 20$, $y = 28$, $z = 20$, area 9/46), middle and inferior temporal gyrus (B; for example $x = \pm 40$, $y = -10$, $z = -22$; $x = \pm 40$, $y = -6$, $z = -46$), frontal eye fields (FEF, [26]; C; $x = \pm 24$, $y = -6$ to 1, $z = 44$ to 51), cerebellum (D; $x = \pm 6$, $y = -52$, $z = -30$) and thalamus (E; $x = \pm 4$, $y = -22$, $z = 8$).

Reconstructed tracts of the left and right putamen projected ipsilaterally to the prefrontal cortex (G; $x = \pm 34$, $y = 46$, $z = -2$, area 10; $x = \pm 34$, $y = 28$, $z = 20$, area 9/46; $x = \pm 28$, $y = 20$, $z = 24$, area8), primary motor area (H; $x = \pm 24$, $y = -16$, $z = 64$),

primary somatosensory area (I; $x = \pm 28$, $y = -32$, $z = 66$, area 1), supplementary motor area (SMA, J; $x = \pm 16$, $y = 16$, $z = 58$), premotor area (K; $x = \pm 28$, $y = -10$, $z = -22$), cerebellum (L; $x = \pm 18$, $y = -56$, $z = -36$) and thalamus (M; $x = \pm 4$, $y = -19$, $z = 2$).

A connectivity-based seed qualification analysis of the caudate showed connections between the DLPFC and the dorsal-posterior caudate and between the VLPFC and the ventral anterior caudate (Fig. 3A).

The connectivity-based seed qualification of the putamen revealed connections between the SMA and dorsal-posterior putamen; premotor areas and medial putamen; and primary motor areas and lateral putamen (Fig. 3B).

Previous anatomical studies in animals have described multiple striatal circuits and suggested that anatomical subcomponents of the striatum, although functionally related, project to distinct cortical areas [7]. In accordance with these studies, we demonstrate several striatal pathways in humans and provide evidence of an anatomical organization between frontal cortex and the caudate nucleus and putamen. More specifically,
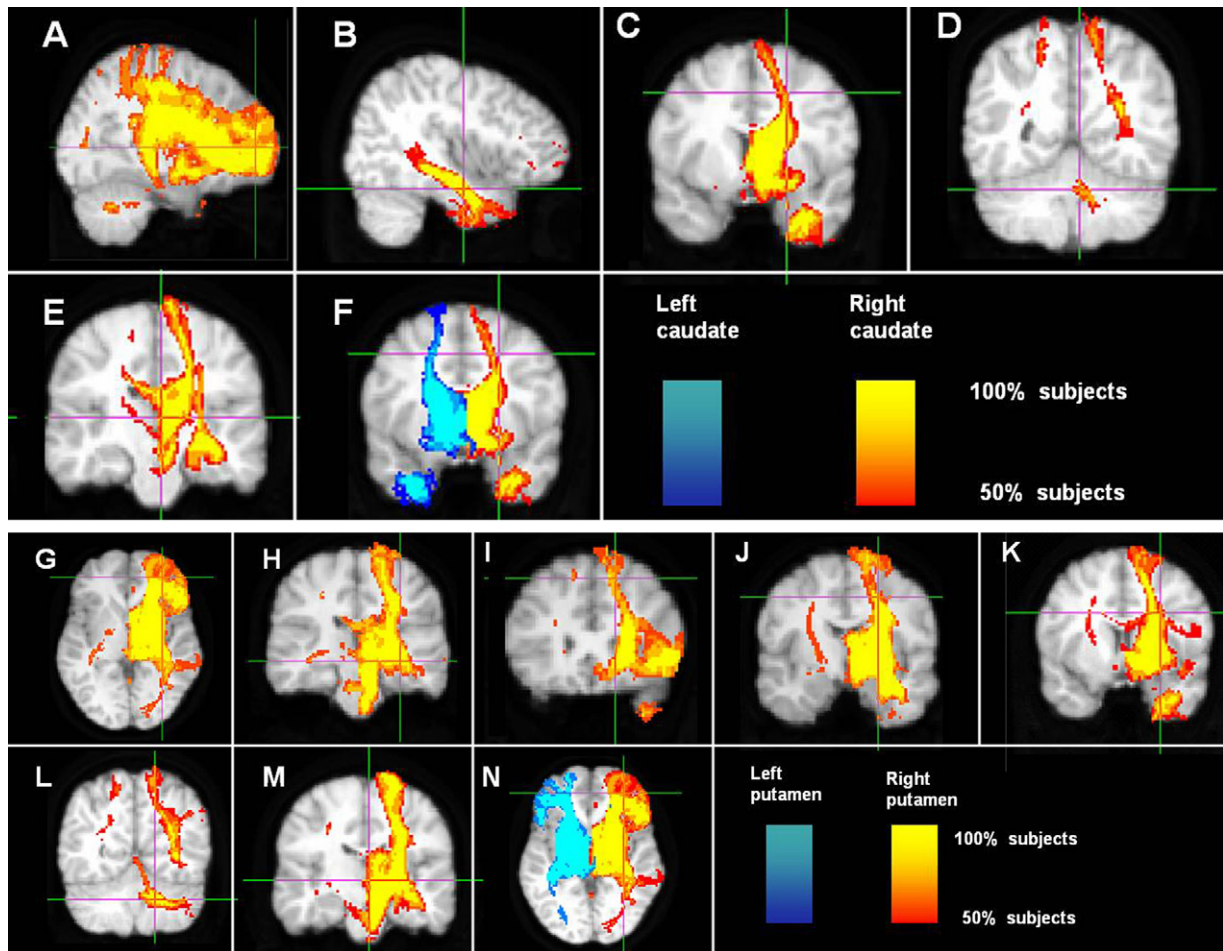
Fig. 2. Illustration of reconstructed left caudate (A–F) and putamen (G–N) tracts. Reconstructed tracts of the left caudate project ipsilaterally to the prefrontal cortex (A), middle and inferior temporal gyrus (B), FEF (C), cerebellum (D), and thalamus (E). The reconstructed tracts of the left putamen project ipsilaterally to the prefrontal cortex (G), primary motor area (H), primary somatosensory area (I), SMA (J), premotor area (K), cerebellum (L) and thalamus (M). Connections of the right caudate and putamen are practically identical (e.g. F, N).

the DLPFC is strongly linked to the dorsal-posterior caudate while the VLPFC is mainly interconnected with the ventral caudate. These results are in keeping with earlier anatomical reports by Yeterian and Pandya [52] suggesting that prefrontal connections are organized topographically.

The confirmation of dorsolateral prefrontal connections to the dorsal-posterior caudate is also consistent with previous functional imaging studies proposing the existence of a 'dorso-lateral prefrontal loop' [11]. A similar observation was made in a repetitive transcranial magnetic stimulation (rTMS) study of the DLPFC that revealed changes in dopamine release specifically in the ipsilateral dorsal caudate nucleus [42].

With regard to the connection between VLPFC and ventral caudate nucleus, corroboration can be found from functional MRI studies during set-shifting tasks [18,19] as well as from anatomical studies in monkeys [40,52].

This organization along a dorsal-ventral axis may be explained by the different functional contributions of these two loops. Several studies have shown that whereas the DLPFC seems to play a part in divided attention and monitoring of information within working memory [12,16,29,32,34,50], the

VLPFC appears to have a specific role in spatial processing [34] and memory retrieval [12,29].

We identified connections between the FEF [26] and the caudate nucleus, in accordance with earlier studies in animals [25,41] and in keeping with the possible involvement of the caudate in oculomotor and saccadic functions [25].

These prefrontal connections may represent the anatomical substrate underlying some of the symptoms associated with neurological (e.g. Parkinson's disease) and psychiatric (e.g. schizoprenia) conditions involving basal ganglia and prefrontal cortex where executive dysfunctions as well as visuospatial dis-orientation have been associated with an impairment of these pathways [18,23,24,33,36].

We also found that reconstructed putamen and caudate fibre tracts projected to the thalamus. Caudate fibre tracts additionally projected to the middle and inferior temporal gyrus, in keep-ing with anatomical studies in animals (e.g. [17]). Middleton and Strick [17] have described striatal-temporal connections and suggested an involvement of the basal ganglia in visual percep-tion where dysfunctional basal ganglia connections may lead to visual hallucinations.
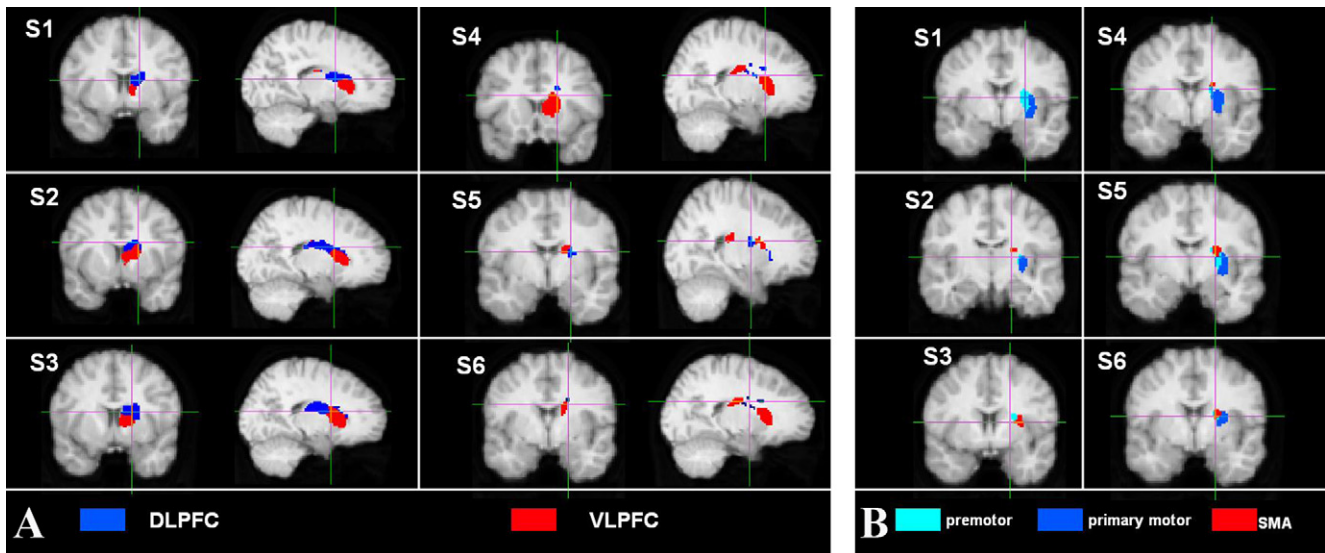
Fig. 3. Connectivity-based seed qualification of the caudate (A) and putamen (B) in all subjects (S1–S6). (A) Connections between DLPFC and dorsal-posterior caudate; VLPFC and ventral anterior caudate. (B) Connections between SMA and dorsal-posterior putamen, premotor area and medial putamen, primary motor area and lateral putamen.

Caudate and putamen pathways to the cerebellum were found to be in accordance with previous anatomical studies in nonhuman primates [8]. Hoshi et al. [8] have suggested that these pathways may modulate basal ganglia activation for adjusting voluntary movements.

With regard to the human putamen, tractography revealed projections to the primary motor area, primary somatosensory area and premotor cortex, all previously described in animal tracing studies and used to explain the involvement of the putamen in motor functions ('sensorimotor circuit', [11]; hyper- and hypokinetic movement disorders, [21,39,46]. More specifically, in keeping with previous observations in nonhuman primates [46], we demonstrate the presence of projections between premotor areas and medial putamen as well as between primary motor area and the lateral putamen in humans. This last observation is in line with a repetitive TMS study of primary motor cortex showing changes in dopamine release in the lateral part of the putamen [43,44]. Furthermore, as is the case in primates [46], we observed connections between dorsal-posterior putamen and SMA.

DTI does not allow differentiating between anterograde and/or retrograde connections. Therefore, we cannot establish whether the delineated pathways are travelling to or from the caudate and putamen. Notwithstanding this limitation, it is our belief that DTI offers great promise to define the organization of anatomical pathway in the human brain and to identify structural abnormalities in various neurological conditions.

In conclusion, reconstructed fiber tracts of the caudate nucleus and putamen appear to project to distinct cortical areas, confirming previous observations in animal studies. The advantage offered by DTI is that it enables the investigation of the prefrontal-basal ganglia loops in humans, a benefit that holds the potential to improve the understanding of the pathophysiology of neurological and psychiatric conditions.

References

[1] G.E. Alexander, M.D. Crutcher, Functional architecture of basal ganglia circuits: neural substrates of parallel processing, Trends Neurosci. 13 (1990) 266–271.

[2] G.E. Alexander, M.R. DeLong, P.L. Strick, Parallel organization of functionally segregated circuits linking basal ganglia and cortex, Annu. Rev. Neurosci. 9 (1986) 357–381.

[3] H. Barbas, D.N. Pandya, Architecture and frontal cortical connections of the premotor cortex (area 6) in the rhesus monkey, J. Comp. Neurol. 256 (2) (1987) 211–228.

[4] M.M. Chakravarty, G. Bertrand, C.P. Hodge, A.F. Sadikot, D.L. Collins, The creation of a brain atlas for image guided neurosurgery using serial histological data, Neuroimage 30 (2) (2006) 359–376.

[5] M.M. Chakravarty, A.F. Sadikot, J. Germann, G. Bertrand, D.L. Collins, Anatomical and electrophysiological validation of an atlas for neurosurgical planning, Med. Image Comput. Comput. Assist. Interv. Int. Conf. Med. Image Comput. Comput. Assist. Interv. 8 (Pt 2) (2005) 394–401.

[6] D.L. Collins, A.C. Evans, ANIMAL: validation and applications of nonlinear registration-based segmentation, Int. J. Patt. Rec. Art. Int. 8 (1997) 1271–1294.

[7] A.T. Ferry, D. Ongur, X. An, J.L. Price, Prefrontal cortical projections to the striatum in macaque monkeys: evidence for an organization related to prefrontal networks, J. Comp. Neurol. 425 (3) (2000) 447–470.

[8] E. Hoshi, L. Tremblay, J. Feger, P.L. Carras, P.L. Strick, The cerebellum communicates with the basal ganglia, Nat. Neurosci. 8 (11) (2005) 1491–1493.

[11] M. Jueptner, C. Weiller, A review of differences between basal ganglia and cerebellar control of movements as revealed by functional imaging studies, Brain 121 (Pt 8) (1998) 1437–1449.

[12] P. Kostopoulos, M. Petrides, The mid-ventrolateral prefrontal cortex: insights into its role in memory retrieval, Eur. J. Neurosci. 17 (7) (2003) 1489–1497.

[13] S.E. Leh, H. Johansen-Berg, A. Ptito, Unconscious vision: new insights into the neuronal correlate of blindsight using diffusion tractography, Brain 129 (Pt 7) (2006) 1822–1832.

[14] S. Lehericy, M. Ducros, A. Krainik, C. Francois, P.F. Van de Moortele, K. Ugurbil, D.S. Kim, 3-D diffusion tensor axonal tracking shows distinct SMA and pre-SMA projections to the human striatum, Cereb Cortex. 14 (12) (2004) 1302–1309.

[16] R. Levy, P.S. Goldman-Rakic, Segregation of working memory functions within the dorsolateral prefrontal cortex, Exp. Brain Res. 133 (1) (2000) 23–32.

[17] F.A. Middleton, P.L. Strick, The temporal lobe is a target of output from the basal ganglia, Proc. Natl. Acad. Sci. USA 93 (1996) 8683–8687.

[18] O. Monchi, M. Petrides, J. Doyon, R.B. Postuma, K. Worsley, A. Dagher, Neural bases of set-shifting deficits in Parkinson's disease, J. Neurosci. 24 (3) (2004) 702–710.

[19] O. Monchi, M. Petrides, A.P. Strafella, K.J. Worsley, J. Doyon, Functional role of the basal ganglia in the planning and execution of actions, Ann. Neurol. 59 (2) (2006) 257–264.

[20] K. Nakano, T. Kayahara, T. Tsutsumi, H. Ushiro, Neural circuits and functional organization of the striatum, J. Neurol. 247 (Suppl. 5) (2000) 1–15.

[21] A. Nambu, K. Kaneda, H. Tokuno, M. Takada, Organization of corticostriatal motor inputs in monkey putamen, J. Neurophysiol. 88 (4) (2002) 1830–1842.

[23] S. Park, P.S. Holzman, Association of working memory deficit and eye tracking dysfunction in schizophrenia, Schizophr. Res. 11 (1) (1993) 55–61.

[24] L. Parnetti, P. Calabresi, Spatial cognition in Parkinson's disease and neurodegenerative dementias, Cogn. Process 7 (Suppl 5) (2006) 77–78.

[25] H.B. Parthasarathy, J.D. Schall, A.M. Graybiel, Distributed but convergent ordering of corticostriatal projections: analysis of the frontal eye field and the supplementary eye field in the macaque monkey, J. Neurosci. 12 (11) (1992) 4468–4488.

[26] T. Paus, Location and function of the human frontal eye-field: a selective review, Neuropsychologia 34 (1996) 475–483.

[27] W. Penfield, K. Welch, The supplementary motor area of the cerebral cortex; a clinical and experimental study, AMA Arch. Neurol. Psychiatry 66 (3) (1951) 289–317.

[28] G. Percheron, C. François, J. Yelnik, G. Fénelon, B. Talbi, The basal ganglia related system of primates: definition, description and informational analysis, in: G. Percheron, J.S. McKenzie, J. Féger (Eds.), The Basal Ganglia IV: New Ideas and Data on Structure and Function, Plenum, New York, 1994, pp. 3–20.

[29] M. Petrides, The mid-ventrolateral prefrontal cortex and active mnemonic retrieval, Neurobiol. Learn. Mem. 78 (3) (2002) 528–538.

[30] M. Petrides, D.N. Pandya, Dorsolateral prefrontal cortex: comparative cytoarchitectonic analysis in the human and the macaque brain and corticocortical connection patterns, Eur. J. Neurosci. 11 (3) (1999) 1011–1036.

[31] M. Petrides, D.N. Pandya, Comparative cytoarchitectonic analysis of the human and the macaque ventrolateral prefrontal cortex and corticocortical connection patterns in the monkey, Eur. J. Neurosci. 16 (2) (2001) 291–310.

[32] Ch. Pierrot-Deseilligny, R.M. Muri, T. Nyffeler, D. Milea, The role of the human dorsolateral prefrontal cortex in ocular motor behavior, Ann. N. Y. Acad. Sci. 1039 (2005) 239–251.

[33] K.M. Prasad, S.D. Sahni, B.R. Rohm, M.S. Keshavan, Dorsolateral prefrontal cortex morphology and short-term outcome in first-episode schizophrenia, Psychiatry Res. 140 (2) (2005) 147–155.

[34] D.S. Rizzuto, A.N. Mamelak, W.W. Sutherling, I. Fineman, R.A. Andersen, Spatial selectivity in human ventrolateral prefrontal cortex, Nat. Neurosci. 8 (4) (2005) 415–417.

[35] S. Robbins, A.C. Evans, D.L. Collins, S. Whitesides, Tuning and comparing spatial normalization methods, Med. Image Anal. 8 (3) (2004) 311–323.

[36] J.M. Rodriguez-Sanchez, B. Crespo-Facorro, R.P. Iglesias, C.G. Bosch, M. Alvarez, J. Llorca, J.L. Vazquez-Barquero, Prefrontal cognitive functions in stabilized first-episode patients with schizophrenia spectrum disorders: a dissociation between dorsolateral and orbitofrontal functioning, Schizophr Res. 77 (2–3) (2005) 279–288.

[37] E.T. Rolls, Neurophysiology and cognitive functions of the striatum, Rev. Neurol. (Paris). 150 (8–9) (1994) 648–660.

[38] M.F. Rushworth, T.E. Behrens, H. Johansen-Berg, Connection patterns distinguish 3 regions of human parietal cortex, Cereb. Cortex 16 (10) (2005) 1418–1430.

[39] J.A. Saint-Cyr, A.E. Taylor, K. Nicholson, Behavior and the basal ganglia, Adv. Neurol. 65 (1995) 1–28.

[40] L.D. Selemon, P.S. Goldman-Rakic, Longitudinal topography and interdigitation of corticostriatal projections in the rhesus monkey, J. Neurosci. 5 (3) (1985) 776–794.

[41] B.L. Shook, M. Schlag-Rey, J. Schlag, Primate supplementary eye field. II. Comparative aspects of connections with the thalamus, corpus striatum, and related forebrain nuclei, J. Comp. Neurol. 307 (4) (1991) 562–583.

[42] A.P. Strafella, T. Paus, J. Barrett, A. Dagher, Repetitive transcranial magnetic stimulation of the human prefrontal cortex induces dopamine release in the caudate nucleus, J. Neurosci. 21 (15) (2001) RC157.

[43] A.P. Strafella, T. Paus, M. Fraraccio, A. Dagher, Striatal dopaimine release induced by repetitive transcranial magnetic stimulation of the human motor cortex, Brain 126 (2003) 2609–2615.

[44] A.P. Strafella, J.H. Ko, J. Grant, M. Fraraccio, O. Monchi, Corticostriatal functional interactions in Parkinson's disease: a rTMS/[11C]raclopride PET study, Eur. J. Neurosci. 22 (11) (2005) 2946–2952.

[45] P.L. Strick, R.P. Dum, N. Picard, Macro-organization of the circuits connecting the basal ganglia with the cortical motor areas, in: J.C. Houk, J.L. Davis, D.G. Beiser (Eds.), Models of Information Processing in the Basal Ganglia, MIT, Cambridge, 1995, pp. 117–130.

[46] M. Takada, H. Tokuno, A. Nambu, M. Inase, Corticostriatal projections from the somatic motor areas of the frontal cortex in the macaque monkey: segregation versus overlap of input zones from the primary motor cortex, the supplementary motor area, and the premotor cortex, Exp. Brain Res. 120 (1) (1998) 114–128.

[47] J. Tanji, The supplementary motor area in the cerebral cortex, Neurosci. Res. 19 (3) (1994) 251–268.

[48] J. Tanji, New concepts of the supplementary motor area, Curr. Opin. Neurobiol. 6 (6) (1996) 782–787.

[50] M. Wagner, T.A. Rihs, U.P. Mosimann, H.U. Fisch, T.E. Schlaepfer, Repetitive transcranial magnetic stimulation of the dorsolateral prefrontal cortex affects divided attention immediately after cessation of stimulation, J. Psychiatr. Res. 40 (4) (2006) 315–321.

[52] E.H. Yeterian, D.N. Pandya, Prefrontostriatal connections in relation to cortical architectonic organization in rhesus monkeys, J. Comp. Neurol. 312 (1) (1991) 43–67.

[53] T.A. Yousry, U.D. Schmid, H. Alkadhi, D. Schmidt, A. Peraud, A. Buettner, P. Winkler, Localization of the motor hand area to a knob on the precentral gyrus. A new landmark, Brain 120 (Pt 1) (1997) 141–157.